Low-Frequency Vibration Actuator Using a DC Motor

Vibol Yem(✉), Ryuta Okazaki, and Hiroyuki Kajimoto

The University of Electro-Communications, Tokyo, Japan
{yem, okazaki, kajimoto}@kaji-lab.jp

Abstract. In our previous study, we found that a normal DC motor can be used for vibro-tactile and pseudo-force presentation. In the present study, we developed a new vibration actuator using a DC motor that can generate much stronger vibrations than a normal DC motor and produce very low frequency of vibrations. We proposed that the stator of the motor could be used as both the vibration mass and fixed rotor of the actuator. To evaluate this design concept, we developed a prototype actuator that can be driven in two modes: stator mode (i.e., the new design concept) and normal mode. The experiment results revealed that stronger vibrations can be obtained on a fingertip in stator mode because the fixed part that comprises the rotor was lighter and the vibration mass using the stator was heavier. We also confirmed that the actuator can be driven at very low frequency (1 Hz) in stator mode.

Keywords: Vibration actuator · DC motor · Low frequency

1 Introduction

Vibration actuators are important for haptic feedback and for simulating tactile experiences. They are currently used in mobile phones, game controllers, and guiding devices for visually impaired persons, to alert or provide environment information to users [1–3]. Eccentric rotation mass (ERM) and linear resonant actuator (LRA) vibration motors are commonly used in these devices because they are small and lightweight, but are still able to produce a strong vibration [4]. However, because of the lack of haptic information, they are not suitable for simulating certain types of tactile experience, such as button clicks [5, 6], heartbeats [7], or the sensation of touching a texture or shape [8, 9]. Successful actuators that are used to provide high-fidelity vibration for tactile experience are the voice coil [10], the Haptuator from Tactile Labs Inc. [11], and the Force Reactor from Alps Electric Co. [12]. These actuators were also found to be able to produce a pseudo-force when the input signal is asymmetric [13–15]. However, they are not suitable for operation in the low-frequency range (e.g., the peak amplitude of vibration is about 100 Hz for the Haptuator and above 200 Hz for the Force Reactor).

In our previous study, we found that a normal DC motor can produce high-fidelity vibration and a pseudo-force, comparable to the voice coil type actuators [16]. The frequency response characteristics were similar to those of the Haptuator when vibrations were applied to a human fingertip, and the peak amplitude was about 40 Hz.

F. Bello et al. (Eds.): EuroHaptics 2016, Part II, LNCS 9775, pp. 317–325, 2016.
DOI: 10.1007/978-3-319-42324-1_31

The advantage of using a DC motor is that it has a potential to produce low-frequency vibrations because the rotor can be used as a vibration mass to rotate infinitely without collision with the stator (i.e., the case of the motor), and it does not have a spring component that is the cause of resonance characteristics.

In the present study, we present a new design concept for a vibration actuator that uses a DC motor which is able to produce strong vibrations than those of a normal DC motor and able to generate low frequency of vibrations (under 10 Hz). We constructed a prototype actuator based on this design and evaluated its performance.

2 Vibration Actuator Using a DC Motor

2.1 Counterforce of a DC Motor

The counterforce of a DC motor is generated on the stator when the rotor is accelerated or decelerated (Fig. 1 (left)). The changing value and direction of the counterforce creates vibrations. The torque, T_r, developed on the rotor and the counterforce, F_s, on the stator can be expressed as follows:

$$T_r = k \times i \tag{1}$$

$$F_s = -\frac{T_r}{R} \tag{2}$$

where k is the torque constant, i is the current flowing in the motor, and R is the radius of the stator.

The mechanical characteristics of a DC motor can be expressed as follows:

$$T_r = J \times \frac{d\omega}{dt} + D \times \omega + F_l \tag{3}$$

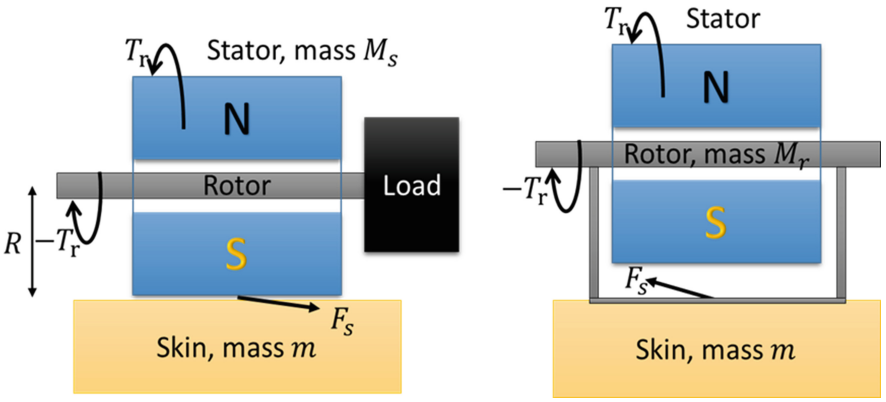

Fig. 1. Schematic for design concept. The stator is fixed and load is added to rotor to obtain high counterforce and smooth movement (left). The rotor is fixed and stator is used instead of load to make the actuator lighter and obtain strong acceleration of skin (right).

where J, ω, and $\frac{d\omega}{dt}$ are the moment of inertia, angular velocity, and angular acceleration of the rotor. D is a viscous friction coefficient and F_l represents the mechanical resistance, such as the internal magnetic loss, which depends on the mechanical characteristics of the motor.

According to Eqs. (2) and (3), to obtain a strong counterforce, we must quickly accelerate the rotor (i.e., produce a high value of $\frac{d\omega}{dt}$). For high-frequency vibration modality, high angular acceleration can be produced by quickly changing the rotational direction of the rotor. However, it is impossible to achieve this at low frequency because acceleration over such a long period will cause the rotor reach to a maximum velocity, at which the acceleration becomes zero, the current is steady (i.e. no load current) and only a very small counterforce is generated as described by the following equations:

$$T_{\mathrm{r}} = D \times \omega + F_l \tag{4}$$

$$F_{\mathrm{s}} = -\frac{D \times \omega + F_l}{R} \tag{5}$$

Moreover, at low frequency of vibration modality, the rotor rotates in high amplitude of angle and due to the changing of orientation of magnetic fields, it produces torque ripple. Torque ripple produces noise and we cannot obtain a smooth movement of rotor [17]. Adding flywheel (load) to the rotor is a classic method to solve these issues (Fig. 1 (left)) [18, 19]. By increasing moment of inertia, J, and energy storage in flywheel, we can reduce the increase of velocity (i.e., the value of $\frac{d\omega}{dt}$ becomes low) and obtain smooth rotation of rotor during acceleration or deceleration. This, however, adds weight to the actuator, which is undesirable for wearable applications, such as a haptic glove. Instead of using flywheel, our idea is using the motor's stator as a load and the rotor as fixed part of actuator because the stator consists of two magnets which are significantly heavier than the rotor (Fig. 1 (right)).

2.2 Amplitude of Skin's Acceleration of a Finger

When the counterforce of the motor, F_{s}, is applied to skin, the skin starts to move with an acceleration, a, that can be expressed as follows (Fig. 1 (right)):

$$a \times (m + M_r) + c \times v + k_{\mathrm{r}} \times x = F_{\mathrm{s}} \tag{6}$$

where v, and x are velocity, and displacement of the skin, respectively. m and M_r are the mass of the skin and the rotor (fixed part), and c and k_r are constants which depend on the stiffness of the skin. Thus, acceleration of the skin can be calculated as follows:

$$a = \frac{F_s - c \times v - k_r \times x}{(m + M_r)} \tag{7}$$

According to the above equation, we can expect to obtain stronger vibration (acceleration is higher) because the mass in the fixed part (M_r) becomes lighter compare to that (M_s) of the case where the stator is fixed.

2.3 Actuator Design

The design figure and prototype of our vibration actuator are shown in Fig. 2. We created a cover and attached it to the shaft of the rotor (Fig. 3 (left)). The cover makes it easy to fix the rotor to the fingertip of a glove (Fig. 4). To allow the stator of the motor to infinitely rotate without the problem of cable winding, we created a secondary brush attached to the cover (the primary brush is inside the DC motor).

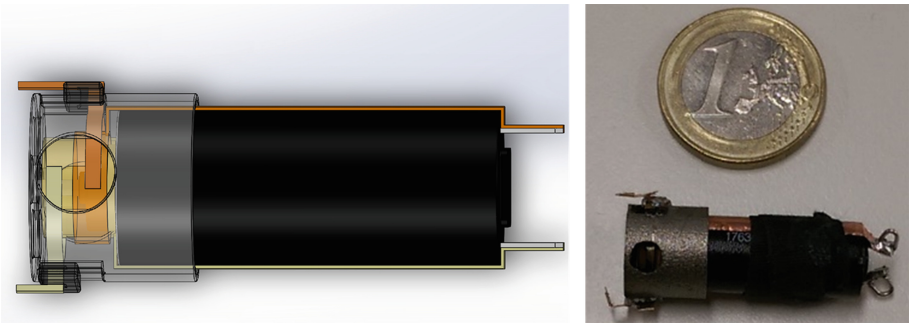

Fig. 2. Design (left) and prototype (right) of the vibration actuator. A cover with a secondary brush was attached to the shaft of the DC motor, which was connected to the rotor.

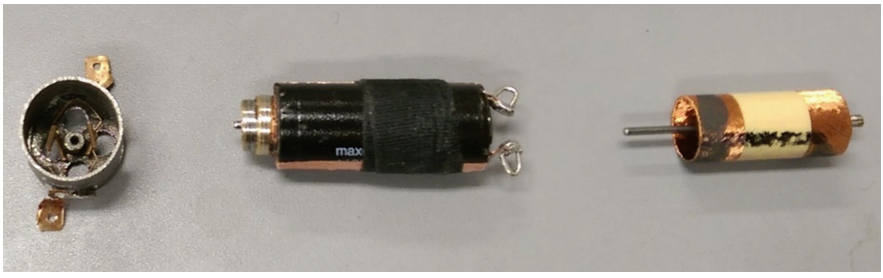

Fig. 3. A cover with a secondary brush (left), the Maxon DC motor (middle), and the rotor coil used in the motor (right).

With this kind of mechanism, we can drive the actuator in either of two modes: normal mode and stator mode. In normal mode, the power supply cables are connected to the primary brush, the cover is free, and the stator is fixed to the fingertip of the glove (Fig. 4 (left)). In this case, the cover is considered as a load and the vibration mass is

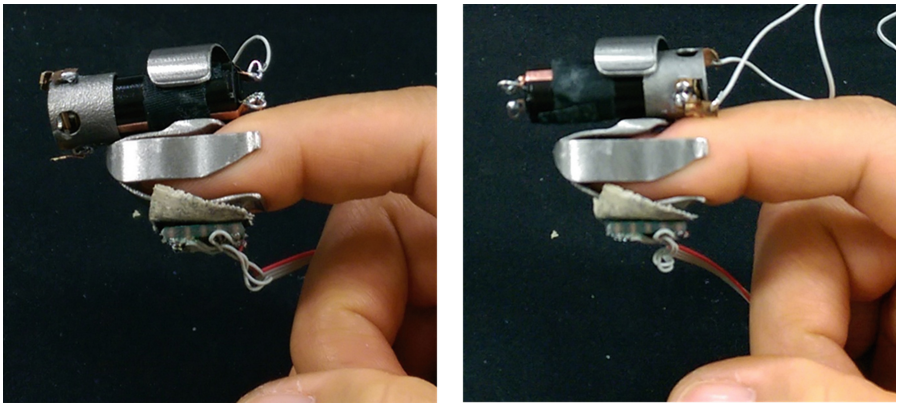

Fig. 4. Vibration actuator operating in normal mode (left) and stator mode (right).

the total mass of the rotor and cover. In stator mode, the power supply cables are connected to the secondary brush, the cover is fixed, and the stator is free and acts as the vibration mass. To obtain stronger vibration in this mode, the mass of the stator needs to be much greater than the total mass of the rotor and cover.

We chose a Maxon DC motor (RE 1.5 W, 118396) for the actuator because its rotor is lightweight, comprising only a coil and a shaft without an iron or steel core (Fig. 3 (right)). In the normal modality of a motor, the lightweight rotor reaches the target rotation angle in a short response time. In the proposed vibration modality, a larger differential mass between the rotor and stator provides a stronger vibration in the stator mode, as demonstrated in the equations above. The total mass of the rotor and cover is just 2 g, which is significantly lighter than the stator (9 g). The actuator is 12 mm × 31 mm in size and has a total weight of 11 g, making it suitable for integration into mobile devices.

3 Evaluation

We experimentally evaluated the proposed design concept and compared the strength of vibration of our prototype actuator in the stator mode to that in normal mode, as detailed in this section.

3.1 Apparatus

To evaluate the actuator vibration, similar to our previous study [16], we opted not to use a mass of 100 g, which is the typical mass used in other studies [4, 10]. Instead, we attached our prototype actuator to the index fingertip of a glove (Fig. 4) to more accurately reproduce a practical situation. The glove was made of titanium and had a weight of 5 g. To observe the vibration on the whole fingertip, the actuator was fixed on the back side and the accelerometer was fixed on the palm side of the finger. Only the index finger of the right hand of the author was used in this evaluation.

A micro-controller (mbed NXP LPC1768) was used to interface with the PC, and to operate the accelerometer (MPU9250, InvenSense; 200 Hz low-pass filter and 1 kHz sampling rate). The input signal was produced by the Pure Data programing software and amplified by an audio amplifier (M50, MUSE Audio Technology). A 1-Ω resistor was serially connected to the actuator to observe the flowing electrical current. An oscilloscope (TDS 1002C-EDU, Tektronix) was used to simultaneously observe the voltage across the actuator and current (a voltage across a 1-Ω resistor) applied to the actuator, and to measure the power (voltage × current) applied to the actuator. To obtain a fairly comparison result, we did not fix the voltage, but fixed the power to 0.3 W for all conditions. We chose low power in this experiment because we wanted to avoid improper vibration due to the rotor reaches to the maximum velocity.

3.2 Procedure

One of the authors sat on a chair and wore the fingertip glove with the accelerometer and actuator in either stator mode or normal mode. During the measurement, the author held their hand on the table in a natural, relaxed position. The input was a sinusoidal wave that ranged from 10 to 200 Hz. The author changed the volume of amplifier to adjust the power supply to 0.3 W for all frequencies. The measurement were conducted five times for each condition.

3.3 Result

In Fig. 5, the frequency response results for each actuator mode are shown. The vertical and horizontal axes represent the amplitude of acceleration and the input frequency,

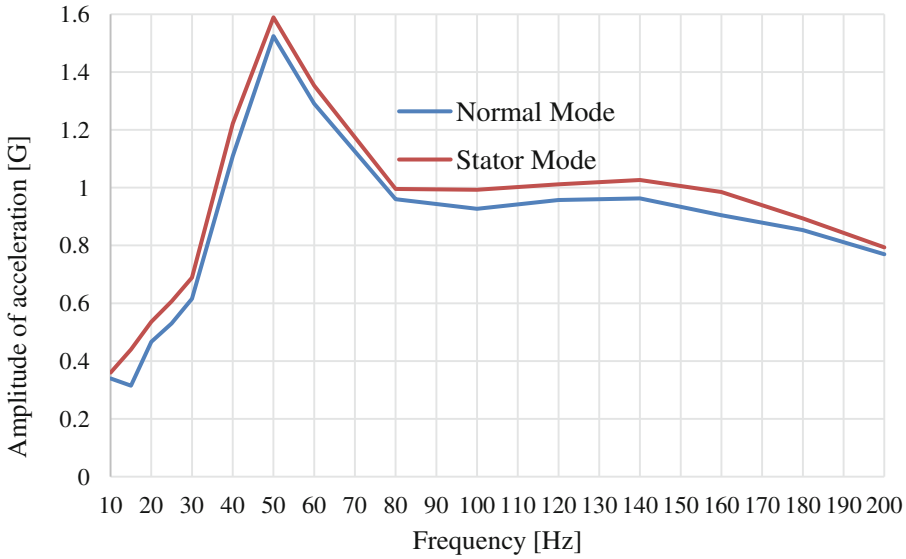

Fig. 5. Frequency response for each mode. (Color figure online)

respectively. The peak amplitude of vibration is at a frequency of 50 Hz for both modes. For almost all frequencies, the vibration amplitude of the stator mode is higher than that of the normal mode.

4 Discussion

The result of the experiment revealed that the stator mode produced a stronger vibration than normal mode for all frequencies. This demonstrates the effectiveness of our design concept. We can explain it by using the Eq. (7). It shows that the acceleration of the skin is inversely proportional to the total mass of the fixed part of the actuator and the skin. In stator mode, the rotor was lighter than the stator. Therefore, the total mass of the fixed part of the actuator was lighter, which generates stronger vibrations than in the normal mode where the stator was fixed.

As mentioned above, the amplitude of vibration also depends on the mass of the skin. In the case that the skin is much heavier than the fixed part and vibration mass, changing from normal mode to stator mode does not give us a stronger vibration. In our experiment, we observed the different of vibration amplitude between the stator mode and normal mode when the device was mounted on the skin of the index finger. We did not conduct a user study to confirm whether the amount of increasing amplitude is detectable. However, this study gave us a clue that to obtain higher percentage difference between the modes, we need to choose a motor with a higher mass ratio of stator to rotor.

In addition to the experiment described above, we tested our prototype at a very low frequency of 1 Hz. For the normal mode, we could not increase the power supply to 1 W despite increasing the voltage to the level of the 9 V (the nominal voltage of the motor is 6 V) because the flowing current was very low. Moreover, the vibration was not smooth, which might be due to the maximum velocity of the rotor. Therefore, it is not suitable to drive it at a very low frequency. By contrast, in the stator mode, we could adjust the power supply to 1 W and obtained smooth sinusoidal motion of vibrations.

We considered that our actuator can also be used to present the sensation of pressure, as it is known that a mechanical receptor of Merkel cell that provides information on pressure is sensitive at low frequency (about 1 to 3 Hz) whereas that of Meissner corpuscle is active at a little higher frequency (about 5 Hz) [20, 21]. To confirm this consideration we asked five participants to wear a fingertip of glove attached with our actuator in stator mode as shown in Fig. 6. We presented 1 W of

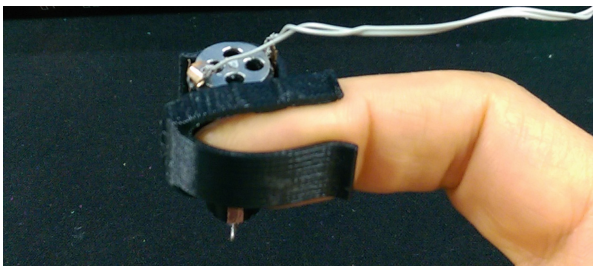

Fig. 6. The actuator was vertically attached to an index finger for providing pushed force sensation by presenting the low frequency (1 Hz) of vibration

power supply and 1 Hz of vibration and asked for their comments. All of them reported that they sensed as if their finger was pushed to move forward and backward but the force pushed from the palm side was stronger.

5 Conclusion and Future Work

The purpose of our study was to develop an actuator that produces strong vibrations at low frequency. We used a DC motor, which we found to be able to provide high-fidelity vibration for this development. According to the design concept, we did not apply a high load to obtain strong vibrations at low frequency, but instead used the stator as a vibration mass. This design has two advantages: the actuator is light and the amplitude of vibration is higher than that of a normal DC motor. To test this design, we created a prototype that can operate in two modes: stator mode and normal mode. Comparative evaluation showed that the vibration strength of the stator mode is higher than that of the normal mode. In our future work, we will develop an algorithm (for a vibration signal at very low frequency) using our actuator to elicit pressure sensation to a human fingertip.

Acknowledgement. This research is supported by the JST-ACCEL Embodied Media Project.

References

1. Wang, Y., Kuchenbecker, K.J.: HALO: haptic alerts for low-hanging obstacles in white cane navigation. In: Proceedings of IEEE Haptics Symposium, pp. 527–532 (2012)
2. Hoggan, E., Brewster, S.A., Johnston, J.: Investigating the effectiveness of tactile feedback for mobile touchscreens. In: Proceedings of the SIGCHI Conference on Human Factors in Computing Systems, pp. 1573–1582 (2008)
3. Pabon, S., Sotgiu, E., Leonardi, R., et al.: A data-glove with vibro-tachtile stimulators for virtual social interaction and rehabilitation. In: Workshop on Presence, pp. 345–388 (2007)
4. Pyo, D., Yang, T.H., Ryu, S., Kwon, D.S.: Novel linear impact-resonant actuator for mobile applications. Sens. Actuators, A **233**, 460–471 (2015)
5. Tashiro, K., Shiokawa, Y., Aono, T., Maeno, T.: A virtual button with tactile feedback using ultrasonic vibration. In: Shumaker, R. (ed.) VMR 2009. LNCS, vol. 5622, pp. 385–393. Springer, Heidelberg (2009)
6. Fukumoto, M., Sugimura, T.: Active click: tactile feedback for touch panels. In: Proceedings of Extended Abstracts on Human Factors in Computing Systems (CHI EA 2001), pp. 121–122 (2001)
7. Nishimura, N., Ishi, A., Sato, M., et al.: Facilitation of affection by tactile feedback of false heartbeat. In: Proceedings of Extended Abstracts on Human Factors in Computing Systems (CHI EA 2012), pp. 2321–2326 (2012)
8. Poupyrev, I., Maruyama, S., Rekimoto, J.: Ambient touch: designing tactile interfaces for handheld devices. In: Proceedings of ACM Symposium on User Interface Software and Technology (UIST 2002), pp. 51–60 (2002)
9. Choi, S., Kuchenbecker, K.: Vibrotactile display: perception, technology, and applications. In: Proceedings of the IEEE, vol. 101, no. 9, pp. 2093–2014 (2013)

10. Yao, H.Y., Haywad, V.: Design and analysis of a recoil-type vibrotactile transducer. J. Acoust. Soc. Am. **128**, 619–627 (2010)
11. Tactile Labs Inc.: http://tactilelabs.com/
12. Alps Electric Co.: http://www.alps.com/e/
13. Amemiya, T., Gomi, H.: Distinct pseudo-attraction force sensation by a thumb-sized vibrator that oscillates asymmetrically. In: Auvray, M., Duriez, C. (eds.) EuroHaptics 2014, Part II. LNCS, vol. 8619, pp. 88–95. Springer, Heidelberg (2014)
14. Rekimoto, J.: Traxion: a tactile interaction device with virtual force sensation. In: Proceedings of ACM Symposium User Interface Software and Technology (UIST), pp. 427–432(2013)
15. Amemiya, T., Ando, H., Maeda, T.: Virtual force display: direction guidance using asymmetric acceleration via periodic translational motion. In: Proceedings of World Haptics Conference, pp. 619–622 (2015)
16. Yem, V., Okazaki, R., Kajimoto, H.: Vibrotactile and pseudo force presentation using motor rotational acceleration. In: Proceedings of Haptics Symposium, pp. 47–51 (2016)
17. Lee, H.H., Qi, W., Kim, S.J., et al.: A simplified torque ripple reduction using the current shaping of the flux swithched reluctance motor. J. Magn. **17**(3), 200–205 (2012)
18. Agrawal, K.C.: Industrial Power Engineering and Applications Handbook. Newnes Press, Boston (2001)
19. Dorrell, D.G., Popescu, M.: Drive motor designs for electric motorcycles. In: Proceedings of IEEE Energy Conversion Congress and Exposition (ECCE), pp. 4354–4351 (2012)
20. Jones, L.A., Lederman, S.J.: Human Hand Function. Oxford University Press, New York (2006)
21. Konyo, M., Tadokoro, S., Yoshida, A., Saiwaki, N.: A tactile synthesis method using multiple frequency vibrations for representing virtual touch. In: Proceedings of Intelligent Robots and System (IROS), pp. 3965–3971 (2005)